Astron. Astrophys. 186, 295–302 (1987)

ASTRONOMY
AND
ASTROPHYSICS

Interstellar clouds: morphological information from projected shapes

M. David and W. Verschueren

Onderzoeksgroep Theoretische Mechanica en Astrofysica, Universiteit Antwerpen (R.U.C.A), Goenenborgerlaan 171, B-2020 Antwerpen, Belgium

Received February 19, accepted June 15, 1987

Summary. The observed image of an interstellar cloud has in general an extremely irregular shape. Nevertheless one can attribute a minor and major dimension (or "axis") to it and construct the distribution of minor to major axis ratios for a given sample of observed cloud images. However irregular the clouds are, one may expect that a morphological characteristic, common to the sampled clouds, will influence this distribution.

The authors propose a statistical procedure to analyse such distributions and show that rough morphological features of the clouds, which can be expressed as correlations between their three dimensions, may in fact be detected.

Key words: data analysis – interstellar medium: clouds: general

1. Introduction

One of the questions which naturally arise in the study of interstellar clouds, is whether anything can be said about the shapes present in a given sample. The answer may be obvious and readily observable as e.g. in the case of supernova remnants or planetary nebulae. But it is not in most other cases.

The question is certainly relevant, for if a sample of observed clouds should prove to exhibit some kind of systematic morphological feature this could, in turn, yield valuable information on the mechanisms which govern the formation and evolution of galactic matter. As an example of such a feature one might think of the oblateness which may result from coupling between a collapsing cloud and a magnetic field which is approximately uniform on the scale of this cloud. Furthermore, since there already exists empirical evidence for a hierarchical structure in the interstellar clouds (the physics governing different scales being distinct from one scale to the next) a method to detect morphological differences between cloud-samples of a different scale, might prove useful.

Obviously our knowledge of samples of giant molecular clouds, cluster associated clouds, etc. which have been mapped hitherto, does not point towards a well defined geometry. Nevertheless, allowing for clumpiness and irregularity of the boundary, it is not inconceivable that there be some kind of correlation between the dimensions of the clouds in a sample. A recent attempt to find such a correlation was made by Leisawitz (1985) who compared the frequency distribution of the ratio of observed minor to major axis-length for a sample of (projected) clouds, with a number of theoretical distributions for this quantity, obtained by assuming that the clouds are spheroids with a minor to major axis ratio within given limits.

In anticipation of a substantial increase of the amount of observational data on interstellar clouds, we discuss here a more general statistical approach. We concentrate on the question to what extent significant conclusions may be drawn from the distribution of observed minor to major axis ratios, but it will be clear that also the distribution of other such crude quantities may be considered and analysed in the same way, if the available data permit it. Although we focus our attention upon interstellar clouds, the procedure we propose may be applied to any other kind of objects (e.g. elliptical galaxies) as well.

2. Definitions

It is convenient to define the dimensions of an arbitrarily shaped 3-dimensional object as the edge-lengths of a box fitted to the object, this box being defined by three couples of parallel planes which touch the object without intersecting it, each couple being normal to the other couples and chosen successively so that the distance between the planes is minimal. The centre of the object may then be defined as the centre of the box. Furthermore we define a Cartesian refernce frame $\boldsymbol{u}_i$, associated to the object, with its origin in the centre, $\boldsymbol{u}_3$ parallel to the major edge and $\boldsymbol{u}_1$ along the minor edge. We will often refer to the dimensions as the "axes" of the object.

The dimensions of the projected shape are defined analogously. This implies that we assume these dimensions to be measured by fitting a rectangle around the projected shape so that the minor edge is minimal.

The calculation of a hypothetical distribution of minor to major axis ratios for the projected shapes of interstellar clouds, to which the observed one can be compared, proceeds as follows. Since obviously the boundary surface of an interstellar cloud cannot be said to belong to a parameter-family of surfaces with a finite number of parameters, one has to select some family of (preferably simple) model shapes (e.g. ellipsoids, boxes, cylinders, ...) to replace the real objects. Of course one has to make sure that this choice does not appreciably affect the final conclusions on a possible correlation between the dimensions. A model family is defined by an equation for the boundary surface:

$$S(x_i, a_j) = 0 \qquad (1)$$

Send offprint requests to: M. David

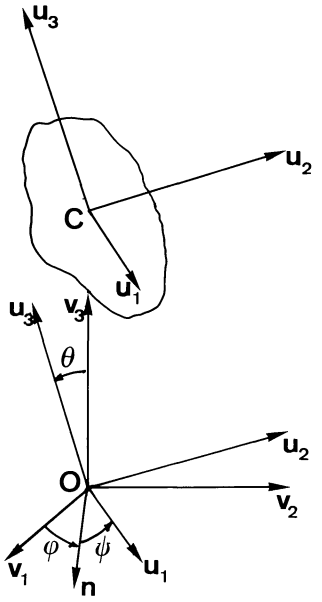

Fig. 1. Illustration of the reference frames and the Eulerian angles; the unit vector $\boldsymbol{n}$ is defined by $\boldsymbol{v}_3 \times \boldsymbol{u}_3 = \boldsymbol{n} \sin\theta$

where $\boldsymbol{x}_i$ represent coordinates in the frame $\boldsymbol{u}_i$ while $a_j (j = 1, \ldots, n)$ are parameters which characterize a particular member of the family (i.e. all shapes in the family may be obtained by varying a_j).

For our purposes an individual model object is completely characterized by its family and by the value of its shape parameters $a_1, \ldots, a_n$, by the position vector $\boldsymbol{r}$ of its centre and by the Euler angles (φ, θ, ψ) of the frame $\boldsymbol{u}_i$ with respect to a Cartesian frame $\boldsymbol{v}_i$ of the observer. This frame is chosen so that $\boldsymbol{v}_3$ points towards the centre of the object (see Fig. 1). A large set of model objects is then described statistically by the function S together with a probability distribution $P_H(a_j; s_k; \boldsymbol{r}, \theta, \psi)$ where s_k are parameters of the distribution such as cut-off values, dispersions, etc. As the dimensions of the projected shapes cannot depend on the azimuthal angle, the latter has been omitted as a variable in the distribution P_H. The composite (S, P_H) will henceforth be referred to as the parent distribution. While a deliberate choice for S is indispensable, of course only P_H is physically relevant as it describes the hypothetical correlation one wishes to examine.

The projection of a given family S onto the plane $(\boldsymbol{v}_1, \boldsymbol{v}_2)$ leads to a family of closed curves contouring the projected model objects. The ratio of minor to major axis of each of these curves is assumed to be known as a function of the shape and the orientation of the objects:

$$R = \Phi(a_j; \theta, \psi), \tag{2}$$

where obviously only θ-values between 0 and $\pi/2$ need to be considered. The reason why this ratio is used rather than the axes themselves is that the ratio does not depend on the position of the object. Noting $W(a_j; s_k; \boldsymbol{r})$ for the statistical weight of a_j and $\boldsymbol{r}$, the distribution of R, corresponding to a given parent distribution is represented as

$$P(R)\,dR = \int_{R < \Phi(a_j;\theta,\psi) < R+dR} P_H(a_j; s_k; \boldsymbol{r}, \theta, \psi) \cdot W(a_j; s_k; \boldsymbol{r})\, da_1 \ldots da_n d^3\boldsymbol{r} \sin\theta\, d\theta\, d\psi \tag{3}$$

in other words, regarding the integration variables as coordinates in a $(n+5)$ dimensional space, $P(R)$ is obtained by integrating over the $(n+4)$ dimensional hyperplane defined by $\Phi(a_j, \theta, \psi) = R$. A normalization factor is assumed to be included in W so that

$$\int_0^1 P(R)\,dR = 1\,. \tag{4}$$

We shall refer to $P(R)$ as the projected distribution.

In general it will be impossible to solve the equation $\Phi(a_j; \theta, \psi) = R$ analytically for one of the variables. Therefore in most cases the integral (3) can be evaluated only numerically. An exception to this is described in the Appendix; it proves to be useful in particular to test a computer program for the numerical calculation. In the examples quoted further on the evaluation of (3) was done by generating a frequency distribution of R-values from randomly chosen sets of values for the integration variables, taking into account their statistical weight. The frequency distribution was then normalized to obtain the probability distribution $P(R)$. In order to guarantee a reasonable convergence of the P-values for classes of width 0.01 in the interval [0,1], at least 10^6 trials were necessary.

3. Features of the projected distribution

3.1. The parent distribution

For the following discussion we consider both ellipsoids and boxes as model objects, the shape parameters being the lengths of the axes, resp. the edges; according to the definition in the previous section these parameters are at once the dimensions of the objects. Without loss of generality we may always assume that

$$a_1 \leqq a_2 \leqq a_3\,. \tag{5}$$

In the case of ellipsoids the projected shapes are obviously ellipses. Noting

$$p = \frac{a_1}{a_3}, \quad q = \frac{a_2}{a_3} \tag{6}$$

the minor to major axis ratio R of these ellipses in the plane $(\boldsymbol{v}_1, \boldsymbol{v}_2)$ is given by

$$R = \sqrt{\frac{F - \sqrt{F^2 - 4G}}{F + \sqrt{F^2 - 4G}}} \tag{7}$$

$$F = p^2 + q^2 + (1 - q^2\cos^2\psi - p^2\sin^2\psi)\sin^2\theta$$

$$G = p^2 q^2 \cos^2\theta + (q^2\sin^2\psi + p^2\cos^2\psi)\sin^2\theta\,.$$

In particular the minor axis x is given by

$$x = a_1 \sqrt{\frac{2G}{p^2(F + \sqrt{F^2 - 4G})}}\,.$$

For a projected box, R is given by different expressions according to the orientation of the box. This leads to a rather cumbersome treatment and it seems preferable simply to project the box and determine the dimensions of the resulting polygon numerically.

The objects are assumed to have a random orientation and a uniform distribution in space, inside a sphere of radius r_m, so the distribution P_H in (3) will be independent of $\boldsymbol{r}$, θ, and ψ. We shall consider the following simple cases of correlation between a_1, a_2, and a_3:

(1) no correlation: the dimensions are uniformly distributed within an interval $[l_-, l_+]$ which, since only ratios are involved, can of course be reduced to $[l_-, 1]$ by expressing all lengths in units l_+; defining

$$I(a_j; l_-) = 1 \quad \text{if } l_- \leqq a_1 \leqq a_2 \leqq a_3 \leqq 1 \\ = 0 \quad \text{otherwise} \tag{8}$$

we have, in the parent distribution:

$$P_H = I(a_j; l_-) \tag{9}$$

(2) oblateness or prolateness: we consider an object as oblate if $a_1 + a_3 < 2a_2$ and as prolate if $a_1 + a_3 > 2a_2$; otherwise the the dimensions are arbitrary within an interval $[l_-, 1]$; so in the parent distribution we now put:

$$P_H = I(a_j; l_-)\, H(2a_2 - a_1 - a_3) \quad \text{(oblate objects)}, \tag{10}$$

or

$$P_H = I(a_j; l_-)\, H(a_1 + a_3 - 2a_2) \quad \text{(prolate objects)}, \tag{11}$$

where H represents the Heaviside function;

(3) preferred dimension ratios: the distribution of the dimensions is such that particular values of p and/or q are much more likely to occur than others; there are many distinct possibilities of this kind, but we shall consider only the following one:

$$P_H = I(a_j; l_-)\ \mathrm{Exp}\left[-\frac{(p-p_0)^2}{2s^2}\right]. \tag{12}$$

3.2. *The statistical weight*

Under the assumptions we made the integration over r may be omitted altogether; taking account of (5) the weight function is then given by

$$W = N_0 \tag{13}$$

where N_0 is a constant ensuring the normalization (4). Since the ratio R depends only on the ratios p and q one might prefer to use these as shape parameters instead of the three dimensions. In that case the weight function becomes

$$W = N_0' \left[1 - \left(\frac{l_-}{p}\right)^3\right]. \tag{14}$$

In practice these expressions may have to be adapted if one knows that the observations are biased in some way, e.g. by decreasing resolution for increasing distance. It is evident that the proper correction factors should be assessed for each particular case, assording to the observation and data reduction techniques one uses. However, as an example we consider the possibility that very narrow objects become unobservable at larger distances because (however long they are) their projected surface does not occupy a sufficiently large solid angle within the detector's beam width. Obviously this will affect the distribution $P(R)$ particularly for small values of R. The appropriate correction factor is obtained as follows.

Suppose that, at the maximal distance r_m, the minor axis of the projected shape should be at least x_l for it to be observable. In that case only a fraction of the objects with minor axis $x < x_l$ will actually be observed; since we have assumed that the objects are distributed uniformly within the sphere r_m, this fraction is $(x/x_l)^3$. Thus the weight function in this case should contain the factor

$$w_{\mathrm{obs}} = H(x - x_l) + \left(\frac{x}{x_l}\right)^3 H(x_l - x). \tag{15}$$

3.3. *Examples*

All projected distributions are normalized so that the surface below the graphs equals one; the probability of finding an R-value in a given class is then obtained by multiplying the functional value with the class width (i.e. 0.01). The small fluctuations of the order of 1% which subsist on all the projected distributions, are due to the fact that we required no better accuracy in the Monte Carlo integration process described in Sect. 2.

3.3.1. No correlation

Contrary to what one might expect, the minor and major axes of the projection of objects with perfectly random dimensions are not at all uniformly distributed (see Fig. 2). Apparently the projection operation itself introduces a certain degree of correlation between minor and major axes of the projected shapes, so one cannot draw any conclusions from the mere fact that a particular set of

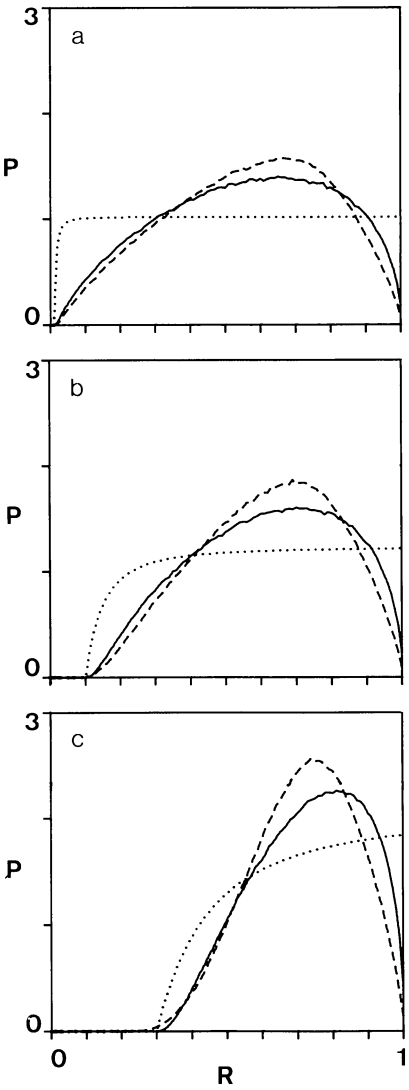

Fig. 2a–c. The projected distribution in the absence of any correlation, obtained using ellipsoids (solid lines) and boxes (dashed lines) as model objects, with **a** $l_- = 0.01$, **b** $l_- = 0.1$, **c** $l_- = 0.3$ in (9). The dotted lines represent the projected distribution one would find if the axes of the projected shapes were themselves uniformly distributed within the interval $[l_-, 1]$

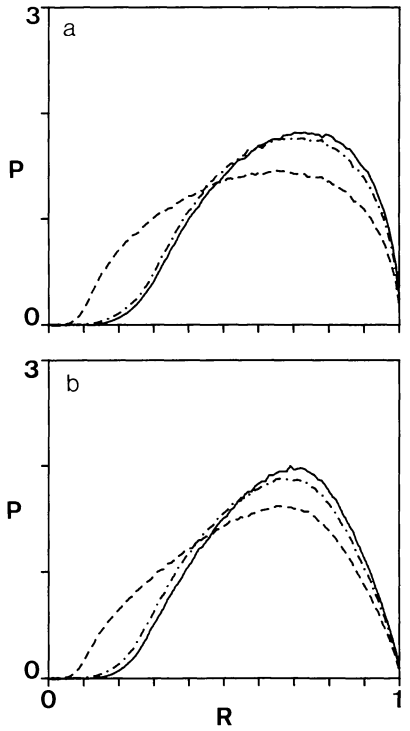

Fig. 3a and b. The projected distribution for a random sample of **a** ellipsoids and **b** boxes, deformed by the bias (15) with respectively: $l_- = 0.01$, $x_l = 0.1$ (dashed lines), $l_- = 0.01$, $x_l = 0.3$ (mixed lines) and $l_- = 0.1$, $x_l = 0.3$ (solid lines)

observed minor and major axes appears to be non-uniformly distributed.

Figure 3 shows the effect of the particular bias described in the previous section. Comparing Figs. 2 and 3 one sees that the overall effect on the projected distributions is quite similar to the effect of varying the parameter l_-, except at the small-R end of the curve which becomes somewhat less steep due to the said bias.

3.3.2. Oblate and prolate objects

Figure 4 compares the projected distributions for oblate and prolate objects respectively. The position of the maximum is markedly different in Figs. 4a and b. Not unexpectedly one finds that prolate objects will more often be seen as oblong shapes while oblate ones will more often appear almost round. This distinction vanishes gradually as the interval of the dimensions $[l_-, 1]$ is reduced.

3.3.3. Preferred dimension ratios

Figure 5 shows some projected distributions for cases where the ratio of the smallest axis of each object to its largest one, has a slightly ($s = 0.5$) or strongly ($s = 0.1$) preferred value. The effect of this kind of correlation on the curves is very much as one expects: for $s = 0.5$ the distribution is practically identical to the corresponding one without any correlation, while for $s = 0.1$ the curves are significantly narrowed in comparison with the corresponding ones in Fig. 2 and the position of the maximum is mainly determined by the parameter p_0.

The hypothesis of "preferred axis ratios" might be dangerous in the sense that, obviously, by varying the parameters p_0 and s, one could fit a "theoretical" projected distribution to almost any observed one which exhibits only a single maximum, while such a fit might not have any physical meaning at all. Therefore this hypothesis (or any other like it) should be considered only if there are theoretical or independent observational reasons to do so.

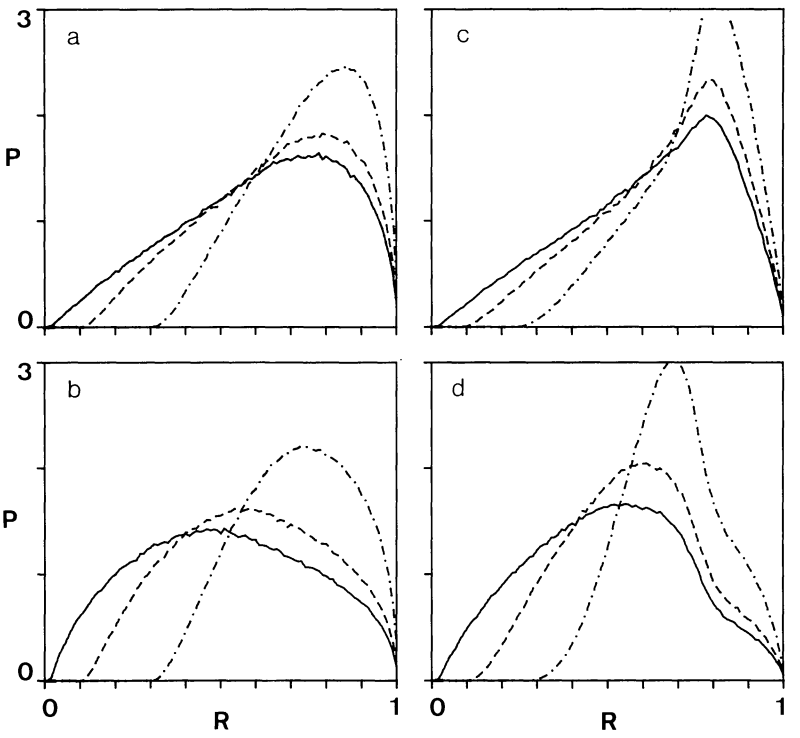

Fig. 4a–d. The projected distribution for **a** oblate ellipsoids, **b** prolate ellipsoids, **c** oblate boxes and **d** prolate boxes; each frame contains the results for $l_- = 0.01$ (solid line), $l_- = 0.1$ (dashed line) and $l_- = 0.3$ (mixed line)

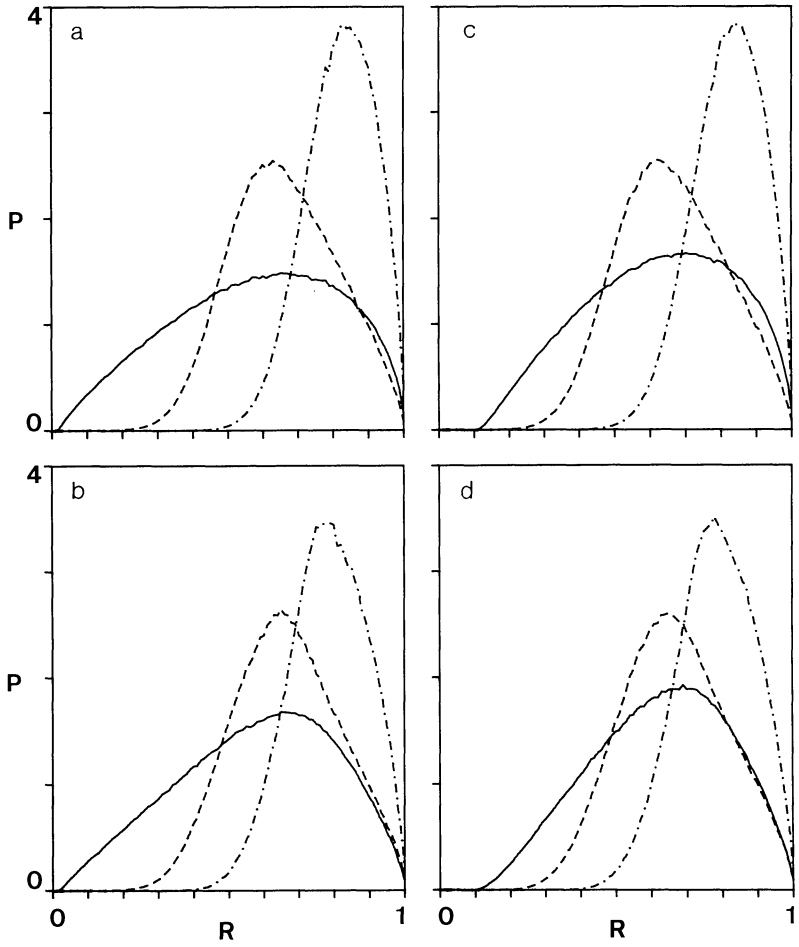

Fig. 5a–d. The projected distribution in different cases of "preferred axis ratios", notably $p_0 = 0.5$, $s = 0.5$, (solid lines), $p_0 = 0.5$, $s = 0.1$ (dashed lines) and $p_0 = 0.75$, $s = 0.1$ (mixed lines); the model objects were **a** ellipsoids with $l_- = 0.01$, **b** boxes with $l_- = 0.01$, **c** ellipsoids with $l_- = 0.1$, and **d** boxes with $l_- = 0.1$

4. Analysis of observed data

4.1. General remarks

The analysis boils down to successively testing a series of hypotheses on the nature of the correlation between the dimensions. The projected distribution corresponding to each hypothesis should be evaluated for several representative values of the parameter l_- since, as the examples show, this parameter strongly affects the shape of the distribution.

The most appropriate test in this case appears to be the Kolmogorov-Smirnov test (see e.g. Lindgren, 1976) which is performed as follows. Let $R_k (k = 1, \ldots, N)$ be a set of observed minor to major axis ratios, arranged in order of ascending magnitude, and $Q_0(R)$ their (cumulative) sample distribution function, i.e.

$$Q_0(R) = \frac{k}{N} \quad \text{for } R_k \leqq R < R_{k+1} \tag{16}$$

with $R_0 = 0$ and $R_{N+1} = 1$. Furthermore let $Q(r)$ be the cumulative distribution corresponding to the hypothetical projected distribution $P(R)$. The K.S. test parameter is then given by

$$T_{KS} = \sup_{\text{all } R} |Q(R) - Q_0(R)| . \tag{17}$$

A hypothesis must be rejected at the α-percent significance level if T_{KS} exceeds a critical value $T_c(\alpha, N)$ which is given in Table 1 for $\alpha = 1, 5$ and for some typical values of N (between which one can interpolate if necessary).

One has to start with testing the hypothesis that there is no correlation. If this hypothesis cannot be rejected at the chosen significance level, one might decide that it is useless to continue the analysis. Nonetheless it could be interesting to test some other hypotheses as well. In particular any hypothesis suggested by

Table 1. Kolmogorov-Smirnov critical values

Sign. level \ N	25	30	35	40	50	60	70	80	90	100	>100
1%	0.32	0.29	0.27	0.25	0.23	0.21	0.19	0.18	0.17	–	$1.63/N$
5%	0.264	0.242	0.23	0.21	0.19	0.17	0.16	0.15	0.14	0.14	$1.36/N$

physical evidence or observational information, is worthwhile to include in the check-list: if it cannot be rejected one must conclude that the observed data are insufficient to verify it, while otherwise at least one has reasons to consider this particular hypothesis as invalid.

It could also be useful to plot the quantity $|Q(R) - Q_0(R)|$ in order to see where the deviation is maximal: knowing qualitatively how the projected distributions change with the variation of certain parameters, it might then be possible to adapt these parameters in the parent distribution in order to obtain a better fit. However, in doing so one should bear in mind that the non-rejection of some hypothesis does in no way imply that it has to be actually accepted, and that one should be extremely careful in drawing conclusions from a "fit" obtained in this way.

4.2. *The selection of model shapes*

We believe that ellipsoids and boxes are actually most convenient to be be used as model shapes in a study of interstellar clouds. From the definition of the dimensions of an object it is obvious that that a given cloud uniquely determines an ellipsoid and a box having the same dimensions and the same centre. The box will enclose the cloud completely while the ellipsoid's surface will generally cut the cloud's surface in many places and will therefore often be closer to a smoothed form of the cloud's surface. Moreover, as long as we know of no constraints whatsoever on the shape of the real objects, there is no sound basis upon which to select a more complicated model and to propose a distribution for its additional shape parameters. However, the question still remains to what extent a hypothetical projected distribution is influenced by the choice of a model shape.

All the examples above reveal that the distribution obtained with boxes as model objects is very much alike to the one obtained with ellipsoids. In particular the rough features such as the position of a maximum, the skewness, etc. are very similar for both families. In other words, these rough features in fact seem to be determined by the distribution of the dimensions of the objects in the population, rather than by their actual shape.

In order to obtain a more quantitative statement on this matter, one can use the K.S.-test parameter as a measure of the distance between two distributions. One can then compare the distance between two projected distributions obtained with the same correlation but a different model family, to the distance between distributions exhibiting different correlations. Table 2 shows the K.S.-test parameters for couples of distributions obtained with ellipsoids or boxes as models for random, oblate and prolate objects respectively (all with $l = 0.01$).

Table 2. The Kolmogorov-Smirnov test-parameter calculated for several couples of theoretical projected distributions as a measure of the distance between the elements of each couple

		Ellipsoids		Boxes		
		Obl.	Pro.	Ran.	Obl.	Pro.
Ellipsoids	Rand.	0.099	0.099	0.029		
	Obl.		0.197		0.026	
	Pro.					0.058
Boxes	Ran.				0.122	0.122
	Obl.					0.244

Even though the distance between ellipsoid-distributions and box-distributions appears to vary strongly according to the nature of the correlation contained in the parent distribution, it does remain appreciably smaller than most distances between two distributions representing a different correlation. We consider this as a justification of the use of simple model shapes to calculate a hypothetical projected distribution, at least for the analysis of relatively small samples for which one may expect the statistical fluctuations to mask any influence due to the actual shape of the observed objects.

The results in Table 2 moreover allow us to estimate for which sample sizes the actual shape of the objects could become relevant to the analysis of an observed distribution. In fact the value of $N_c = (1.36/T_{KS})^2$ can be considered as an estimate for the sample size necessary to be able to distinguish the two distributions between which T_{KS} is the distance. Considering the largest T_{KS}-value between corresponding distributions for boxes and ellipsoids in Table 2 we find $N = 550$. For sample sizes well below this number the influence of the true cloud-shapes on the observed distribution may be considered as irrelevant to the analysis discussed here.

Finally it should be noticed that the danger of biasing the analysis by the use of a simple model shape is reduced if one makes no statistical decision unless the test results obtained using boxes, agree with those obtained using ellipsoids.

4.3. *Example*

The axis lengths published by Leisawitz are not really fit for an application of the procedure outlined above, since they were measured in a way which is different from the one assumed in Sect. 2. Therefore the use we make here of these data – no other similar data having been published to our knowledge – is merely illustrative.

From the set of clouds described by Leisawitz we first selected those which were completely mapped as well as possibly or probably associated to some cluster; the result is a sample of 67 objects; its cumulative minor to major axis distribution is shown in Fig. 6. Using this observed distribution three hypotheses were tested: (a) the dimensions are completely random (i.e. no correlation), (b) the clouds are oblate, and (c) the clouds are prolate. The test results are summarized in Table 3.

First of all we notice that the test-parameter values for boxes are in reasonable agreement with those for ellipsoids, so that it is in fact possible to draw conclusions which are independent of the

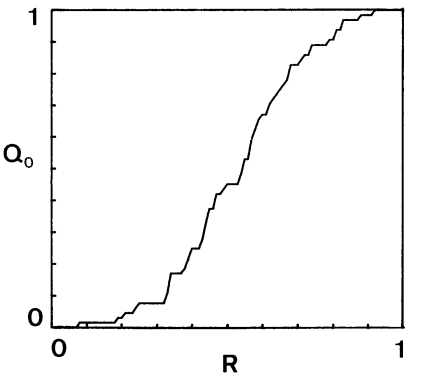

Fig. 6. The cumulative distribution of minor to major axis ratios for a sample of 67 images of clouds which are probably or possibly associated to an open cluster, based upon data from Leisawitz (1985)

Table 3. Values of the Komogorov-Smirnov parameter testing different hypotheses against the observed distribution for the set of 67 selected objects

Hypothesis/model	l_-	0.01	0.05	0.1	0.15	0.3
(a)	Ellipsoid	0.175	0.204	0.244	0.289	0.452
	Box	0.163	0.193	0.233	0.276	0.439
(b)	Ellipsoid	0.258	0.285	0.321	0.360	0.499
	Box	0.283	0.316	0.358	0.400	0.524
(c)	Ellipsoid	0.177	0.122	0.167	0.218	0.412
	Box	0.150	0.087	0.114	0.186	0.398

model shape used. According to the critical values listed in Table 1, hypothesis (a) must be rejected at the 5% significance level (though not at the 1% level) and hypothesis (b) must be rejected even at the 1% significance level. The results for (c) are peculiar in that the test parameter, viewed as a function of l_-, exhibits a distinct minimum in the vicinity of $l_- = 0.05$. Clearly there is a range of l_--values, common for both model shapes, in which hypothesis (c) cannot be rejected (at least on the basis of the axis lengths published by Leisawitz).

The same tests were performed on a sample of 40 non-cluster-associated objects (completely mapped as well as incompletely mapped); the results are shown in Table 4.

For this sample hypothesis (b) must again be rejected at the 5% significance level (though not anymore at the 1% level if $l_- = 0.01$ is considered), while (a) cannot be rejected at all, as contrasted with the previous sample. These two points of difference may be ascribed to the fact that the sample size is smaller, since they also appear in an arbitrary subsample of 40 objects picked from the set of cluster-associated clouds (see Table 5). However, one also sees that the testparameter now exhibits a minimum under hypothesis (a) as well as under (c), and that the minimum of T_{KS} under hypothesis (c) is shifted towards a higher value. The same differences are found between Table 4 and Table 5 so they point at an essential difference between the observed distributions for the two kinds of objects.

Table 4. Values of the K.-S.-parameter for a sample of 40 non-cluster-associated clouds

Hypothesis/model	l_-	0.01	0.05	0.1	0.15	0.3
(a)	Ellipsoid	0.226	0.183	0.217	0.273	0.448
	Box	0.206	0.177	0.231	0.287	0.448
(b)	Ellipsoid	0.224	0.253	0.293	0.335	0.473
	Box	0.249	0.285	0.328	0.369	0.474
(c)	Ellipsoid	0.294	0.235	0.164	0.211	0.423
	Box	0.268	0.204	0.134	0.205	0.422

Table 5. Values of the K.S.-parameter ofr a subsample ($N=40$) of the sample considered in Table 3

Hypothesis/model	l_-	0.01	0.05	0.1	0.15	0.3
(a)	Ellipsoid	0.136	0.165	0.205	0.259	0.413
	Box	0.124	0.169	0.227	0.281	0.406
(b)	Ellipsoid	0.220	0.246	0.283	0.322	0.460
	Box	0.244	0.277	0.320	0.362	0.485
(c)	Ellipsoid	0.177	0.117	0.146	0.218	0.394
	Box	0.149	0.094	0.171	0.245	0.404

5. Conclusions

It is possible to detect certain morphological characteristics of interstellar clouds in the form of crude correlations between their dimensions, from a statistical analysis of the distribution of the minor to major axis ratios of the projected cloud-shapes which one observes. The analysis requires the introduction of simple model shapes for the clouds, but this arbitrary element will not bias the results of the analysis for sample sizes well below 500; only for higher sample sizes the introduction of more realistic model shapes might become meaningful.

Acknowledgements. The authors are indebted to H. Hensberge for several stimulating discussions and useful suggestions, and to C. de Loore for a critical reading of the manuscript.

Appendix

If the parametric family of model shapes is limited to spheroids, the integral (3) can be evaluated analytically under the circumstances assumed in Sect. 3.1, in case there is no correlation and in case the correlation is prolateness or oblatenes. We consider now the latter two cases.

For prolate spheroids one has $a_1 = a_2 < a_3$ so that $p = q$; substituting this in (3) we get

$$R^2 = \frac{p^2}{p^2 \cos^2\theta + \sin^2\theta} \tag{A1}$$

and thus

$$\cos\theta = \frac{1}{R}\sqrt{\frac{R^2 - p^2}{1 - p^2}}, \quad p \leqq R, \quad 0 \leqq \theta \leqq \frac{\pi}{2}. \tag{A2}$$

In (3) the integration over ψ and $\boldsymbol{r}$ may be omitted, and the integration over a_1 and a_3 replaced by an integration over p which is the only essential shape parameter left; (A2) describes the curve Γ in (p, θ) space along which the integral is to be taken. Assuming $l_- = 0$ and $l_+ = 1$, the weight function is now simply $W = 1/(p_1 - p_0)$, where the bounds $p_0 \leqq p \leqq p_1$ can be used to introduce the additional correlation of "limited axis ratios" (otherwise $p_0 = 0$, $p_1 = 1$). Equation (3) then becomes:

$$P(R)\,dR \begin{cases} = 0 & \text{for } R < p_0 \\ = \dfrac{1}{(p_1 - p_0)} \int_\Gamma \sin\theta\, d\theta\, dp & \text{for } p_0 \leqq R \leqq 1\,. \end{cases} \tag{A3}$$

Eliminating θ by means of (A2) we obtain in the latter case:

$$P(R)\,dR = \frac{dR}{(p_1 - p_0)} \int_{p_0}^{\mathrm{Min}(R,p_1)} \frac{p^2\,dp}{R^2\sqrt{(R^2-p^2)(1-p^2)}}$$

and eventually, noting $p_* = \mathrm{Min}(p_1, R)$:

$$P(R) = \frac{1}{(p_1 - p_0)\,R^2} \cdot \left\{F_1\left(R, \frac{p_*}{R}\right) - E_1\left(R, \frac{p_*}{R}\right) - F_1\left(R, \frac{p_0}{R}\right) + E_1\left(R, \frac{p_0}{R}\right)\right\}, \quad p_0 \leqq R \leqq 1\,, \tag{A4}$$

where F_1, E_1 represent Jacobi's form of the elliptic integrals of the first and second kind respectively.

For oblate spheroids we must put $a_2 = a_3$ so that $q = 1$. Substituting this in (3) we get

$$F = (1+p^2) + (1-p^2)\sin^2\theta\sin^2\psi$$
$$G = p^2 + (1-p^2)\sin^2\theta\sin^2\psi \tag{A5}$$

With the definitions we adopted throughout, the symmetry axis of the oblate spheroids is $\boldsymbol{u}_1$, and its angle γ with the axis $\boldsymbol{v}_3$ of the observer is given by

$$\cos\gamma = \sin\psi\,\sin\theta, \quad 0 \leqq \gamma \leqq \frac{\pi}{2}, \quad 0 \leqq \psi \leqq \frac{\pi}{2}. \tag{A6}$$

So

$$R^2 = 1 - (1-p^2)\sin^2\gamma\,. \tag{A7}$$

In (3) the integration over ψ cannot be omitted anymore, but γ can be substituted for ψ by means of (A6); one has in particular

$$d\psi = \frac{-\sin\gamma\,d\gamma}{\sqrt{\sin^2\gamma - \cos^2\theta}} \qquad \cos\theta \leqq \sin\gamma\,.$$

Replacing again the integration over a_1 and a_3 by an integration over p, the integral in (p, γ, θ)-space has to be taken along the plane Σ defined by (A7), i.e.

$$\cos\gamma = \frac{R^2 - p^2}{\sqrt{1-p^2}}, \quad p \leqq R \leqq 1\,. \tag{A8}$$

Thus

$$P(R)\,dR \begin{cases} = 0 & \text{for } R < p_0 \\ = \dfrac{-2}{(p_1 - p_0)\pi} \int_\Sigma \dfrac{\sin\theta\sin\gamma\,d\theta\,d\gamma\,dp}{\sqrt{\sin^2\gamma - \cos^2\theta}} & \text{for } p_0 \leqq R \leqq 1\,. \end{cases} \tag{A9}$$

After integrating over θ ($\arccos(\sin\gamma) \leqq \theta \leqq \pi/2$), eliminating γ by (A8) and integrating over p ($p_0 \leqq p \leqq p_* = \mathrm{Min}(R, p_1)$) one finds

$$P(R) = \frac{R}{(p_1 - p_0)} \left\{F_1\left(R, \frac{p_*}{R}\right) - F_1\left(R, \frac{p_0}{R}\right)\right\}, \quad p_0 \leqq R \leqq 1\,. \tag{A10}$$

References

Leisawitz, D.T.: 1985, Molecular clouds associated with young open star clusters, Ph.D. Thesis, The University of Texas at Austin

Lindgren, B.W.: 1976, Statistical Theory, MacMillan, New York